Importance of local structural distortions in magnetocaloric effect in Mn based antiperovskites

2016 J. Phys.: Conf. Ser. 712 012117

(http://iopscience.iop.org/1742-6596/712/1/012117)

Journal of Physics: Conference Series **712** (2016) 012117 doi:10.1088/1742-6596/712/1/012117

Importance of local structural distortions in magnetocaloric effect in Mn based antiperovskites

K R Priolkar[1,*], E T Dias[1], G Aquilanti[2], Ö Çakir[3], M Acet[4], A K Nigam[5]

[1]Department of Physics, Goa University, Taleigao Plateau, Goa 403206 India
[2]Elettra-Sincrotrone Trieste S.C.p.A., s.s. 14, km 163.5 I-34149 Basovizza, Trieste, Italy
[3]Physics Department, Yildiz Technical University, TR-34220 Esenler, Istanbul, Turkey
[4]Faculty of Physics and CENIDE, Universitat Duisburg-Essen, D-47048 Duisburg, Germany
[5]Tata Institute of Fundamental Research, Dr. Homi Bhabha Road, Colaba, Mumbai 400005, India

E-mail: krp@unigoa.ac.in

Abstract. Mn_3GaC and Mn_3SnC are two antiperovskites which exhibit a large magnetocaloric effect associated with a magnetostructural transformation. Although structurally similar, the magnetic transition and the nature of magnetocaloric effect in the two compounds is completely different. While Mn_3GaC transforms from a ferromagnetic to an antiferromagnetic state at $T_t = 178$K with the antiferromagnetic propagation vector along $k = \frac{1}{2}, \frac{1}{2}, \frac{1}{2}$, in Mn_3SnC the transformation occurs at $T_t = 280$K from a paramagnetic state to an antiferromagnetic state with $k = \frac{1}{2}, \frac{1}{2}, 0$. Mn K EXAFS has been employed to show that these differences in magnetic properties are related to local structural distortions in Mn_6C octahedra which are quite different in the two compounds.

1. Introduction

A class of materials that have attracted attention as candidates for ferroic cooling applications are the Mn based antiperovskite materials. Amongst these Mn_3GaC undergoes a volume discontinuous first order transition from a ferromagnetic (FM) to an antiferromagnetic (AFM) ground state around 160K [1, 2] accompanied by a large inverse table like magnetocaloric effect (MCE) in relatively low fields especially preferred in designing a practical refrigerant unit [3, 4]. On the other hand, isostructural Mn_3SnC exhibits a sharp first order change from a paramagnetic (PM) state to a non-collinear antiferromagnetic state at 279K accompanied by a conventional magnetic entropy change (80.69 mJ/cm^3-K under a magnetic field of 2T) [2, 5].

Although both the samples undergo a cubic-cubic phase transformation, neutron diffraction studies have shown that the antiferromagnetic propagation vector k in the two compounds is different. In Mn_3GaC, k is along $\frac{1}{2}, \frac{1}{2}, \frac{1}{2}$ direction [6] while Mn_3SnC orders with $k = \frac{1}{2}, \frac{1}{2}, 0$ which makes two of the three Mn atoms to order antiferromagnetically while the third one has a small ferromagnetic component along the z direction [7]. There are however, no signatures of any structural disorder that could explain this difference in magnetic behavior. In order to check for any local structural disorder, Mn K edge EXAFS studies were performed across the first order transition on Mn_3GaC and Mn_3SnC compounds. Our study reveals presence of such

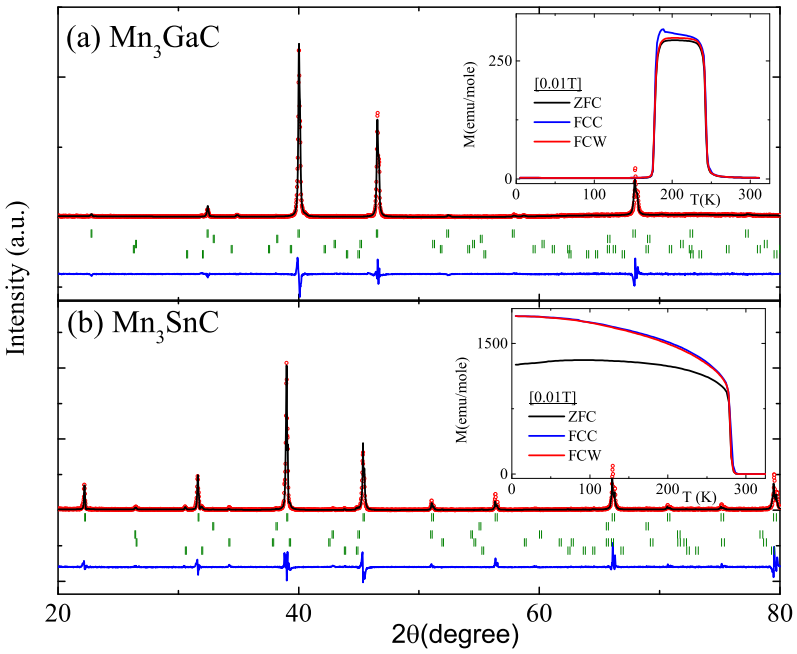

Figure 1. Rietveld refined X-ray diffraction patterns recorded for (a) Mn_3GaC and (b) Mn_3SnC at room temperature. Insets in the respective panels show temperature evolution of magnetization recorded during ZFC, FCC and FCW cycles.

a disorder that could be related to the observed differences in the magnetic properties of the two compounds.

2. Experimental

The compounds used here were prepared by solid state reaction method, details of which are given in Ref. [8] and characterized by x-ray diffraction (XRD) and magnetization as a function of temperature during the zero field cooling (ZFC), field cooled cooling (FCC) and field cooled warming (FCW) cycles. Extended x-ray absorption fine structure (EXAFS) data at the Mn K edge (6539 eV) was collected in transmission mode at 300K (RT) and 80K (LT) in the range from -200 to 1300 eV with respect to the Mn K edge at the XAFS beamline at Elettra, Trieste [9]. The data was processed using Demeter program [10].

3. Results and Conclusions

Rietveld refined XRD patterns recorded in the angular (2θ) range of 20° to 100° in steps of 0.02° using Cu K_α radiation are presented in Figure 1 and show the formation of cubic antiperovskite phase for both the compounds along with minor impurity phases ($\sim 1\%$).

Magnetization (M) of Mn_3GaC, recorded as a function of temperature under ZFC, FCC and FCW conditions at an applied field of 0.01T (see inset of Figure 1a) exhibits a PM to FM transition at T_C = 242K followed by a FM to AFM first order transition at T_t = 178K [11]. Mn_3SnC on the other hand exhibits a single transition depicted by a sharp increase in magnetization at T_t = 280 K (inset of Figure 1b) which corresponds to a first order transition from a high temperature low volume PM state to a low temperature high volume magnetically ordered phase with competing FM and AFM interactions [7].

k weighted Mn K edge EXAFS data in R space and back transformed k space recorded

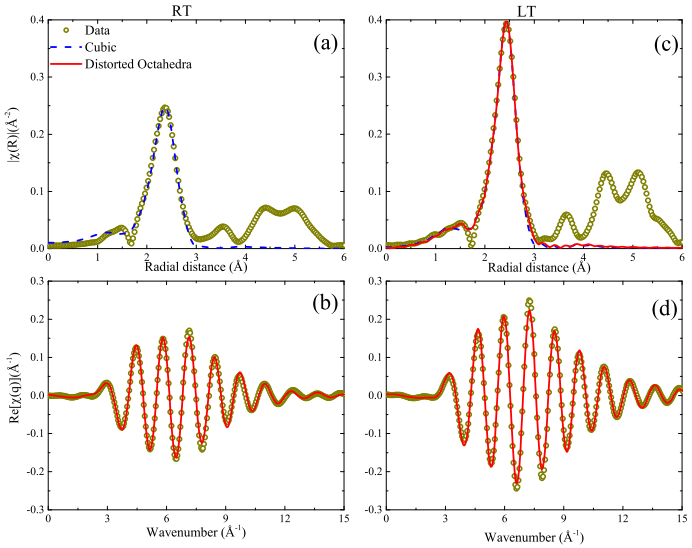

Bond	R_{XRD}	R_{EXAFS}
RT		
Mn-C	1.949	1.923(4)
Mn-Mn	2.757	2.720(6)
Mn-Ga	2.757	2.720(6)
LT		
Mn-C	1.943	1.937(3)
Mn-Mn	2.748	2.779(5)
Mn-Ga	2.748	2.735(2)

Figure 2. EXAFS spectra in R space ((a) and (c)) and Fourier filtered k space ((b) and (d)) at RT and LT in Mn_3GaC. The dashed lines and the solid lines indicate best fit for cubic and distorted octahedra model respectively. The table gives the best fitted values of bond lengths from XRD and EXAFS.

at RT and LT for Mn_3GaC and Mn_3SnC are presented in Figures 2 and 3 respectively. While Mn_3GaC EXAFS data at RT could be well fitted to a model incorporating structural constraints (shown as a dashed line (cubic model) in Figure 2(a)), satisfactory fits could not be obtained for Mn_3SnC EXAFS data recorded at both, RT and LT using this model (Figure 3(a) and (c)). Similarly, the cubic model, though fitted well (dashed line in Figure 2(c)) to the LT data of Mn_3GaC, gave some unphysical parameters (mean square relative displacements, $\sigma^2 < 0$). Therefore, the structural constraints were relaxed and bond distances and σ^2 for each scattering path were varied independently. The resulting fit is shown as a solid line (distorted octahedra) in Figure 2(c). The fitted values of bond distances are listed in a table alongside the Figure 2. It can be seen that, at LT, the Mn–C and Mn–Ga distances slightly shorten while Mn–Mn bonds elongate. This situation corresponds to a rhombohedral distortion of the cubic unit cell in the transformed phase. The AFM ground state of Mn_3GaC is believed to be due to increased Mn–C hybridization. The shorter Mn–C bond distance obtained here agrees well with this hypothesis. The RT and LT data in the Fourier filtered space along with best fits are presented in Figures 2(b) and (d) respectively.

In the case of Mn_3SnC, it was found that local structure of Mn consists of a distribution of shorter and longer bond distances (distorted octahedra model). While about 2/3 of Mn–C and Mn–Mn bonds shorten and the rest grow longer. In the case of Mn–Sn distances the distribution was exactly reversed. Such a local structural distortion though preserves the overall cubic symmetry, distort the Mn_6C octahedra so as to elongate along one direction and compress along other two. The best fits to the data in R space are shown as solid lines in Figure 3(a) and (c) and the back transformed data at RT and LT along with the best fits are shown in Figure 3(b) and (d) respectively. The best values of bond distances obtained are listed in a Table alongside the Figure 3.

These distortions of Mn_6C octahedra agree well with the observed propagation vector k and

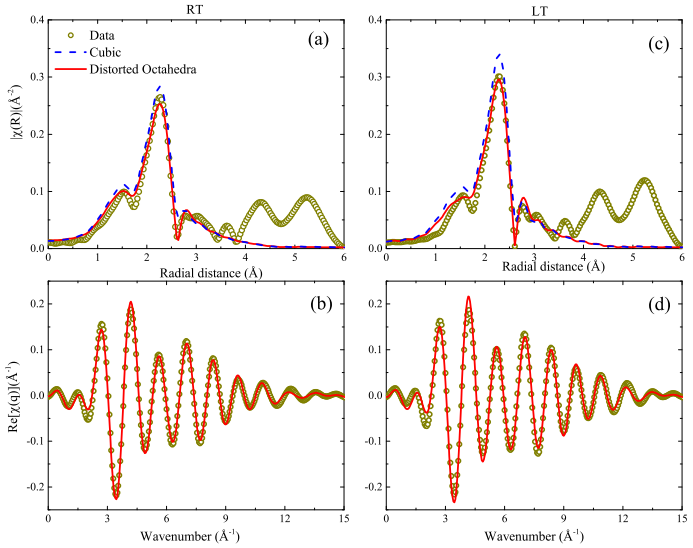

Bond	R_{XRD}	R_{EXAFS}
RT		
Mn-C	1.998	2.032(2)x0.33 1.958(2)x0.67
Mn-Mn	2.826	2.874(2)x0.33 2.769(2)x0.67
Mn-Sn	2.826	2.874(2)x0.67 2.769(2)x0.33
LT		
Mn-C	1.997	2.029(3)x0.33 1.961(3)x0.67
Mn-Mn	2.824	2.869(3)x0.33 2.773(3)x0.67
Mn-Sn	2.824	2.869(3)x0.67 2.773(3)x0.33

Figure 3. R space ((a) and (c)) and back transformed k space ((b and (d)) EXAFS spectra recorded at RT and LT for Mn_3SnC. The dashed lines and the solid lines indicates best fit with cubic and distorted octahedra model respectively. The table gives the best fitted values of bond lengths from XRD and EXAFS.

the observe MCE. In Mn_3GaC, the octahedra are distorted along [111] direction so also is the antiferromagnetic alignment of Mn spins resulting in an inverse MCE [6]. While, in Mn_3SnC the elongation of octahedra along one direction is perhaps responsible for the antiferromagnetic alignment of two of the three Mn atoms and a pure ferromagnetic moment on the third [7]. This pure ferromagnetic moment explains the conventional MCE in Mn_3SnC.

Acknowledgments

Financial support by Board of Research in Nuclear Sciences (BRNS) under the project 2011/37P/06 is acknowledged.

References

[1] Bouchaud J, Fruchart R, Pauthenet R, Guillot M, Bartholin H and Chaiss F 1966 *J. Appl. Phys.* **37** 971–972 URL `http://scitation.aip.org/content/aip/journal/jap/37/3/10.1063/1.1708544`

[2] Fruchart D and F Bertaut E 1978 *Journal of the Physical Society of Japan* **44** 781–791 URL `http://dx.doi.org/10.1143/JPSJ.44.781`

[3] García J, Bartolomé J, González D, Navarro R and Fruchart D 1983 *J. Chem. Thermodyn.* **15** 1059 – 1069 URL `http://www.sciencedirect.com/science/article/pii/0021961483900319`

[4] Tohei T, Wada H and Kanomata T 2003 *J. Appl. Phys.* **94** 1800–1802 URL `http://scitation.aip.org/content/aip/journal/jap/94/3/10.1063/1.1587265`

[5] Wang B S, Tong P, Sun Y P, Luo X, Zhu X B, Li G, Zhu X D, Zhang S B, Yang Z R, Song W H and Dai J M 2009 *Europhys. Lett.* **85** 47004

[6] Ö Çakir, Acet M, Farle M and Senyshyn A 2014 *J. Appl. Phys.* **115** 043913 URL `http://scitation.aip.org/content/aip/journal/jap/115/4/10.1063/1.4862903`

[7] Dias E T, Priolkar K R, Das A, Aquilanti G, akir, Acet M and Nigam A K 2015 *Journal of Physics D: Applied Physics* **48** 295001 URL `http://stacks.iop.org/0022-3727/48/i=29/a=295001`

[8] Dias E T, Priolkar K R and Nigam A K 2014 *Mater. Res. Express* **1** 026106 URL `http://stacks.iop.org/2053-1591/1/i=2/a=026106`

[9] Cicco A D, Aquilanti G, Minicucci M, Principi E, Novello N, Cognigni A and Olivi L 2009 *J Phys Conf Ser* **190** 012043
[10] Ravel B and Newville M 2005 *J Synchrotron Radiat* **12** 537–541
[11] Dias E, Priolkar K and Nigam A 2014 *J. Magn. Magn. Mater.* **363** 140 – 144 URL http://www.sciencedirect.com/science/article/pii/S0304885314002807